environmental and earth sciences proceedings

MDPI

Proceeding Paper

Towards an Operational Forecast Model Suite for Compound Inundation Due to Flash Floods and Storm Tides in Coastal Areas with Non-Perennial Rivers †

Angelos Kokkinos [1,*], Christos V. Makris [2], Yannis Androulidakis [3], Zisis Mallios [1], Ioannis Pytharoulis [4], Theophanis Karambas [1] and Yannis N. Krestenitis [1]

[1] Department of Civil Engineering, Aristotle University of Thessaloniki, 54124 Thessaloniki, Greece; zmallios@civil.auth.gr (Z.M.); karambas@civil.auth.gr (T.K.); ynkrest@civil.auth.gr (Y.N.K.)
[2] Department of Civil Engineering, Democritus University of Thrace, 67100 Xanthi, Greece; cmakris@civil.duth.gr
[3] Department of Marine Sciences, University of the Aegean, 81100 Mytilene, Greece; iandroul@aegean.gr
[4] Department of Geology, Aristotle University of Thessaloniki, 54124 Thessaloniki, Greece; pyth@geo.auth.gr
* Correspondence: angeloks@civil.auth.gr
† Presented at the 9th International Electronic Conference on Water Sciences, 11–14 November 2025; Available online: https://sciforum.net/event/ECWS-9.

Abstract

This study presents a two-dimensional hydraulic modelling framework for the simulation of flash and compound flooding in coastal urban areas with non-perennial river systems. The model employs a rain-on-grid approach within HEC-RAS v6.7 beta5 (2D solver) to simulate rainfall-driven runoff and explicitly incorporates coastal water-level forcing to represent storm tides. The framework is applied to an ungauged coastal basin in northern Greece using a 50-year return period design storm. Model results show good agreement with official Flood Risk Management Plan maps while identifying additional inundated areas linked to lower-order streams. Compound flooding simulations indicate a 21% increase in flooded areas, highlighting the importance of integrated modelling for operational flood forecasting.

Keywords: compound flooding; flood modelling; hydraulic modelling; rain-on-grid; HEC-RAS 2D; operational flood forecasting; coastal zone; storm tide

1. Introduction

In recent years, the frequency of floods has increased due to human interventions in the natural environment and the impacts of climate change. Urbanisation within river floodplains has intensified community exposure to flood risk. Additionally, coastal zones influenced by non-perennial river systems face an elevated risk of flooding due to the combined effects of pluvial events, fluvial overflows, and storm surges, a situation further aggravated by climate change and uncontrolled urbanisation. Particularly hazardous because of their rapid onset are flash floods, which are triggered by intense rainfall over short periods.

To simulate such phenomena, 2D hydrodynamic models are widely used for flood extent mapping because they yield more detailed and reliable results for complex flow simulations. Additionally, 2D models can simulate the timing and duration of inundation with adequate accuracy [1–3]. A further step in these models is the inclusion of spatial rainfall information via the rain-on-grid (RoG) method [4–6]. In this approach, rainfall is

Academic Editor: Hossein Bonakdari

Published: 12 March 2026

applied directly to each cell of the two-dimensional hydraulic model, thereby simulating surface runoff without requiring an intermediate hydrological model to convert precipitation into runoff. The main advantage of this method is its ability to physically simulate the catchment's hydrological behaviour rather than estimate parameters using conventional hydrological approaches. However, the method is associated with both hydraulic and hydrological limitations.

The RoG approach has been widely investigated in recent years within HEC-RAS 2D and other hydrodynamic solvers. Previous studies have shown that the hydraulic performance of RoG simulations may exhibit artificial terrain-storage effects, leading to peak attenuation and delayed runoff response, particularly for short-duration storm events. These numerical artefacts are closely related to grid resolution and can be mitigated through mesh refinement [4,6]. Benchmarking analysis by Costabile et al. [7] reported generally satisfactory performance of HEC-RAS 2D in real-world urban and catchment-scale applications, while highlighting numerical sensitivity in the treatment of wet-dry fronts and shallow overland flow conditions. It has further been emphasised that the occurrence of shallow flows may require calibration of roughness coefficients, as these can deviate from standard values typically adopted in fluvial flood simulations [8,9]. From a hydrological perspective, other studies have shown that RoG models are well-suited for single-event flash floods but exhibit limitations for long-duration or multi-peak events due to simplified infiltration routines and the absence of subsurface return flow [6,9,10]. For the non-perennial Mediterranean catchments considered here, where flow initiation is dominated by infiltration-excess and rapid surface routing, rain-on-grid formulations offer a physically consistent alternative to hydrograph-based coupling, particularly under operational time constraints.

This study builds upon the established rain-on-grid methodology by implementing it within an operational forecasting-oriented modelling framework for a Mediterranean coastal basin characterised by non-perennial streams and urban fabric. Specifically, the novelty lies in the implementation of the RoG method focusing on: (i) the explicit integration of rainfall-driven flash flooding with coastal water-level forcing within a unified 2D domain, and (ii) the systematic evaluation of grid resolution and computational performance to ensure operational applicability. The aim is to forecast flash floods using available meteorological precipitation data, as part of an integrated framework for simulating and forecasting compound flooding in the Thermaikos Gulf, northern Greece [11].

2. Data and Methods

2.1. Study Area

The study area consists of the coastal zone east of the Thermaikos Gulf, extending from Thessaloniki International Airport to the town of Agia Triada, and includes the urban fabric of Peraia (Figure 1). The study area is classified as a Flood Risk Zone according to the Flood Risk Management Plan (FRMP) of the Central Macedonia Water District [12]. It features a well-developed hydrographic network, with the Livadaki torrent (1st order network in Figure 1) as the main channel, located between the airport and the urban area of Peraia, and a series of second- and third-order streams that run transversely across the entire coastal urban area.

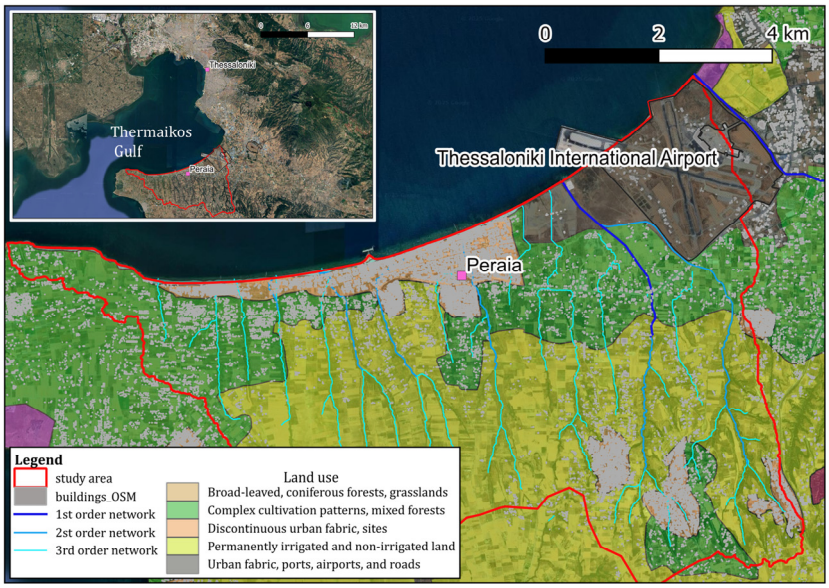

Figure 1. Map of the study area. The map depicts the land-use classes used to select roughness coefficients, the area's hydrographic network, and buildings in urban and semi-urban areas.

2.2. Data

The digital elevation model (DEM) for the catchment is provided by the National Cadastre of Greece, with a spatial resolution of 2 × 2 m^2. The DEM was checked and corrected where necessary, particularly in areas near bridges along the main and the secondary streams. In addition, buildings in urban areas, which are shown in Figure 1, were represented as solid objects, within which flow is excluded. This is achieved by locally increasing the DEM elevation for each building, so that the terrain corresponding to constructed artefacts is particularly higher than the surrounding bare earth. Land-use data obtained from the CORINE Land Cover system, with a spatial resolution of 30 × 30 m^2. Figure 1 also shows the land uses of the area, where the CORINE Land Cover classes were merged into a reduced number of land-use categories according to their assigned Manning's roughness values, in order to simplify the parameterisation of surface roughness. These data indicate that the study area is predominantly agricultural, with permanently irrigated and non-irrigated croplands covering nearly half of the total area (49.7%), followed by complex cultivation patterns and mixed forest–shrub formations, which together account for 28.2%. Urban land uses, including continuous and discontinuous urban fabric, transport infrastructure, ports, and airport facilities, represent a substantial share (21.4%), reflecting the strong influence of urbanisation. Marine areas occupy a negligible proportion of the study area (0.7%). The Manning's coefficients assigned to each land use category follow the detailed work of [13] on hydraulic modelling of coastal inundation and were set to 0.012, 0.018, 0.040, and 0.140 for continuous urban fabric, discontinuous urban fabric, arable land, and complex cultivation patterns-mixed forests, respectively.

The storm event used in this study corresponds to a 50-year return period. To derive the design hyetograph (Figure 2) of the total precipitation, the available intensity–duration–frequency (IDF) curves for the study area were used. The IDF curves have been developed at the national scale within the framework of implementing the EU Floods Directive (2007/60/EC) [14]. The design storm duration is 48 h, in accordance with the FRMP for this area.

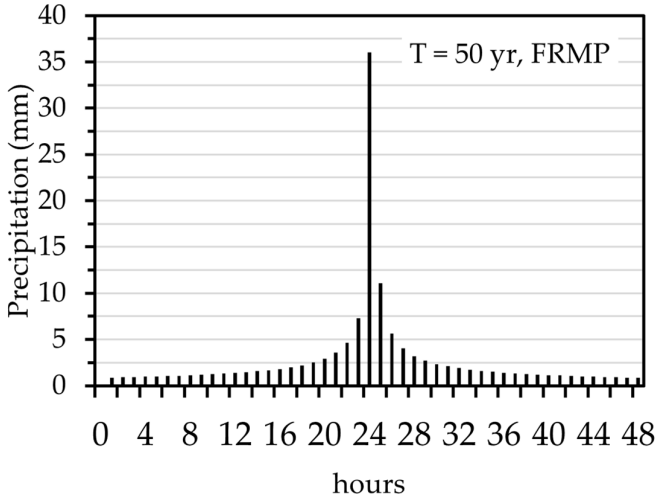

Figure 2. Hourly hyetograph for the simulated design storm, corresponding to a 50-year return period.

The Soil Conservation Service–Curve Number (SCS–CN) method [15] was used to estimate effective rainfall from total precipitation; it is used exclusively to estimate effective rainfall volumes and does not represent flow routing or storage, which are entirely resolved by the 2D hydraulic solver. This method does not account for soil and groundwater storage; therefore, it is suitable for simulating single-storm events. The effective rainfall is derived from the total rainfall, subtracting the precipitation loss as:

$$I = \frac{(P - \lambda S)^2}{(P + S - \lambda P)}, \; S = \left(\frac{25,400}{CN}\right) - 10 \quad (1)$$

where I is the accumulated precipitation excess in mm, P is the accumulated precipitation depth, λ is the initial abstraction rate equal to 0.2, and S is the maximum soil retention in mm. CN is defined spatially based on the CN map developed during the first revision of the area Flood Risk Management Plan of the area [11]. CN values selected refer to normal antecedent moisture conditions (AMC II). Dry-channel conditions were assumed, as there is no baseflow in the streams. Although detailed information on the urban drainage network was not available to explicitly account for its dynamic response, its impact was approximated by assuming a constant minimum infiltration rate of 0.22 mm h^{-1}, applied uniformly across the urban areas.

2.3. Methods

The hydraulic simulations were performed using the HEC-RAS v6.7 beta 5 (U.S. Army Corps of Engineers, Hydrologic Engineering Center, Davis, CA, USA) model [16], applying the Diffusion Wave equations (DW). The computational domain covers the entire study area to account for rainfall over its full extent. Boundary conditions were applied only as outflow conditions at the limits of the computational domain. No inflow conditions were imposed, as rainfall is introduced as a source term in each computational cell. As a downstream boundary condition, when coastal flooding is considered, a uniform total seawater depth was specified along the entire coastline. At this stage, the coastal boundary condition represents a still-water level of 0.98 m, corresponding to the 50-year return level scenario of the updated FRMP [12] (represents a static storm-tide envelope, not dynamic surge propagation). When only precipitation-driven flash flooding is considered, a normal-depth boundary condition is applied at the downstream boundary, with appropriate longitudinal slopes defined locally according to the area's topography.

Since the model is intended to be operational, reducing computational runtime is a key objective, which primarily depends on the size of the computational mesh. Simulations

were therefore performed using bulk grid resolutions of Δx = 100 m, 50 m, and 25 m. Figure 3 illustrates the mesh configuration for a bulk grid with Δx = 50 m. The local refinement region in the coastal urban area and the break-lines along the main stream channels are indicated. These refinement zones employed cell sizes of 20 m, 10 m, and 5 m, depending on the grid-sensitivity scenario examined. Therefore, the mesh configurations considered consist of bulk resolutions (100/50/25 m) combined with local refinements (20/10/5 m) in the areas of interest.

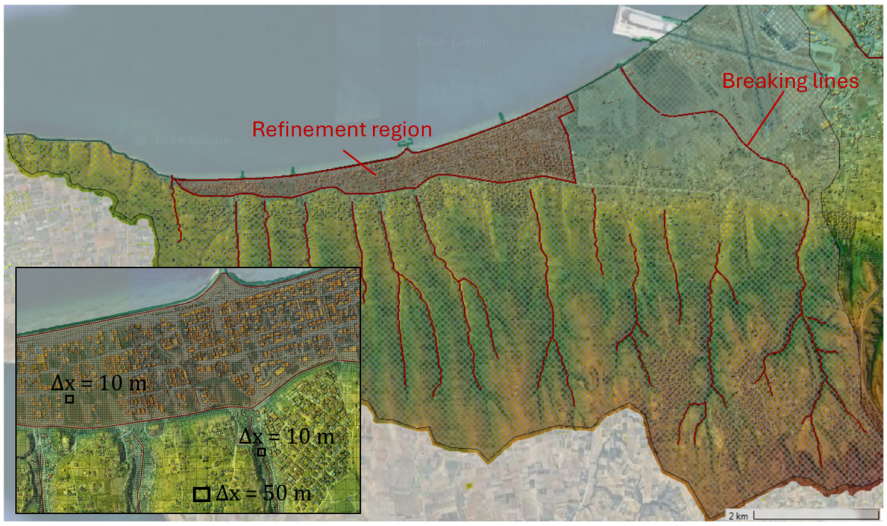

Figure 3. Computational mesh with bulk cell size Δx = 50 m, showing the refinement region (Δx = 10 m) in the coastal urban area and the break-lines (Δx = 10 m) along the main stream channels.

3. Results and Discussion

The simulations were performed using the DW formulation, which requires significantly lower computational cost compared to the full Shallow Water Equations (SWE). This choice was made because the present model is developed for operational applications, where the emphasis is on the timely production of actionable flood information for early warning rather than on a detailed representation of the dynamic behaviour of the flood wave. It is acknowledged that, for rapidly varying flash floods, the full SWE formulation, including local and convective acceleration terms, may be required to capture the detailed flood hydrodynamics.

A necessary condition for adopting the DW formulation is verification that it can reproduce the study's target variable with sufficient accuracy, namely, the maximum flood extent. To assess this, a comparison between simulations using the DW and SWE formulations is presented in Figure 4. Figure 4a shows the maximum flooded area for three water depth thresholds, indicating that the differences between the two approaches are very small (<1%). Furthermore, Figure 4b presents a representative section of the inundation map in the urban area of Peraia, where the green boxes indicate the areas with the largest differences between the two simulations. It is shown that the spatial differences between the two formulations are negligible for the purposes of the present study.

Although the study area is prone to both coastal and flash flooding, it is an ungauged catchment for which no flood events are recorded in remote sensing data. This makes the direct validation of the computational model challenging. The only available reference results for the area are those provided by the FRMP, which show flooding due to precipitation produced through two-dimensional hydrodynamic simulations using design hydrographs for the main watercourses. For coastal inundation, the FRMP's assessment of coastal flood extent used a static 'bathtub' approach with hydraulic connectivity, approx-

imating inundation as areas with ground elevations less than or equal to the estimated sea level rise corresponding to a given return period. Beyond the application of good modelling practices, as described in the EU Floods Directive framework, the reliability of these flood maps is further enhanced by a formal consultation process with local authorities, professional engineers, and the public, through which local knowledge and experience were incorporated. Consequently, comparing our model results with the FRMP flood maps provides a benchmark indicating that the developed model achieves an accuracy comparable to that used in official governmental flood risk management actions.

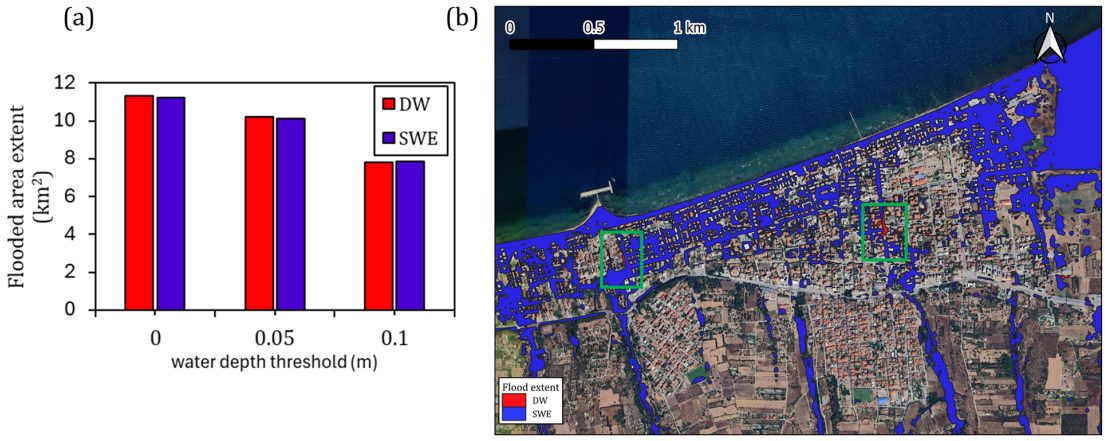

Figure 4. Comparison of flood extent obtained with the Diffusion Wave (DW) and Shallow Water Equations (SWE) formulations. (**a**) Flooded area for different water depth thresholds; (**b**) spatial distribution for a threshold of 0.0 m. Green boxes indicate areas with the largest differences between the DW–SWE simulations.

Figure 5a presents the flood-extent map from the FRMP for the study area, based on a 50-year return-period design hydrograph for the Livadaki stream. The map includes all wet cells (water depth > 0.0 m) according to the FRMP definition of inundation. To reduce sensitivity to wet–dry numerical tolerance, we also verified that the comparative patterns remain unchanged for other literature-based practical depth thresholds (e.g., >0.05 m and >0.10 m), consistent with Figure 4. The figure also shows the flood extent for the same storm event obtained with the RoG model at a 25 × 25 m^2 mesh resolution, considering only fluvial/pluvial flooding. The comparison indicates that the flood extent simulated by the RoG model is larger than that depicted in the FRMP maps. This difference is attributed to the distinct representation of surface runoff in the two modelling approaches, highlighting the advantage of the RoG method in areas characterised by numerous small streams. The additional inundated areas identified by the RoG simulation originate primarily from spatially distributed runoff generation and the activation of second- and third-order channels, which are not explicitly represented in hydrograph-based FRMP modelling. This highlights the importance of spatial rainfall representation in urbanised coastal basins with dense ephemeral drainage networks. The RoG model successfully captures the entire flooded area identified in the FRMP maps, achieving a hit rate of 92%, while also identifying areas flooded by lower-order streams or by direct rainfall accumulation (i.e., interpreted as pluvial-dominated flooding rather than overestimation). A representative example is the airport area, where the largest discrepancy between the two flood maps is observed. The FRMP map shows a smaller flooded area originating solely from the Livadaki stream, whereas the RoG model indicates more extensive flooding from rainfall directly over the airport area. Although the airport has been treated as an urban area with extensive impervious surfaces, information on its surface drainage system is classified; therefore, the model results for this area cannot be considered fully accurate.

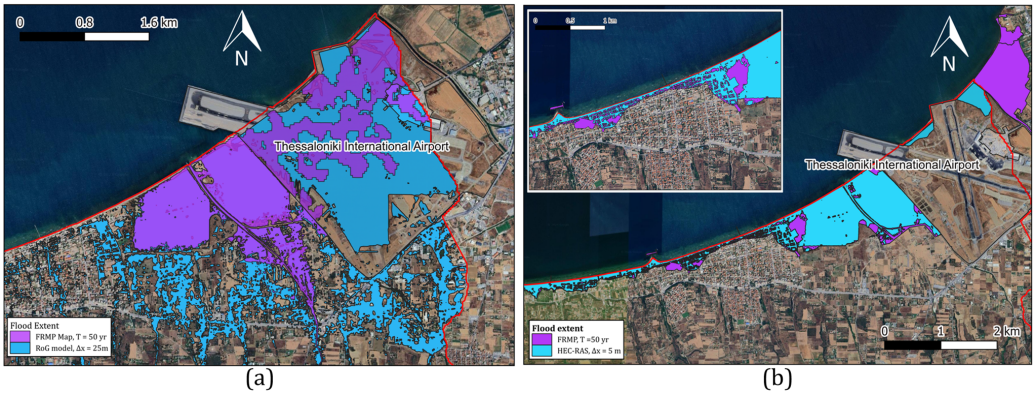

(a) (b)

Figure 5. (**a**) Fluvial/pluvial flood extent comparison for a 50-year return period event: FRMP vs. RoG model (25 × 25 m^2 mesh). (**b**) Coastal flood extent comparison for a 50-year return period event: FRMP vs. HEC-RAS model (5 × 5 m^2 mesh). The red line indicates the study area boundary.

Figure 5b shows the comparison between the coastal flood extent (water depth > 0.0 m) estimated within the framework of the FRMPs and the extent computed by the present simulations at a grid resolution of Δx = 5 m in the coastal area. The simulated inundation extent is largely consistent with that of the FRMPs, both around the Livadaki stream and in the urban area of Peraia (Figure 5b inset map). It should be noted, however, that the FRMP-derived flood extents inherently reflect structural uncertainties associated with the underlying methodological assumptions, such as hydrograph-based routing schemes and simplified "bathtub" approaches for coastal inundation. Consequently, the comparison presented herein should be interpreted as a comparison between two distinct modelling frameworks rather than a validation against observations. The inundated area derived from the simulations is more limited than that of the FRMPs, which is attributed to both the inclusion of buildings in the simulations and, more importantly, to the more detailed computational approach adopted, which renders the results more reliable.

Finally, Figure 6 compares the maximum flood extent maps from the rainfall-only and compound flooding scenarios to assess the contribution of each flooding source to the final inundation. In this simulation, a 10 m grid is used in the urban areas and the stream channels, and a 50 m grid for the rest of the area. The results indicate that the additional flooded area resulting from the inclusion of storm tide (viz., meteorological surge and astronomical tide oscillations) amounts to 21% and is observed not only along the coastal waterfront but also within the urban interior.

Figure 6. Comparison of the flood extent map between the compound flooding and the precipitation-only scenarios. The green color represents the overlap of the yellow and blue colors from the precipitation-only and compound flooding maps, respectively. The red line indicates the study area boundary.

Although detailed information, such as flood depth and velocity, is particularly valuable for the design of risk management measures, this study focuses on evaluating the flood extent map, which is often sufficient for operational modelling purposes when available in a timely manner. Comparing the flood extent map for the examined grid resolutions due to precipitation, it is found that the model with a $\Delta x = 25$ m mesh produces the largest flood extent, while simulations with $\Delta x = 50$ m and 100 m reproduce 93% and 88% of this extent, respectively. For these simulations, the ratio T_{sim}/T_{com} equals 27.6, 22.6, and 5.95 for grid resolutions of $\Delta x = 100$ m, 50 m, and 25 m, respectively (Figure 7), where T_{sim} denotes the simulation scenario duration (48 h) and T_{com} the actual computational time. All simulations were performed on an AMD Ryzen 9 7950X 16-Core Processor (4.50 GHz) (Advanced Micro Devices, Santa Clara, CA, USA), utilising all cores permitted by the HEC-RAS architecture (8 cores). For a simulation to be considered suitable for operational use, the ratio should be less than 6, thereby allowing timely intervention. Under the given hardware configuration, even the simulation with a $\Delta x = 25$ m mesh marginally satisfies this constraint. For coastal flooding, the grid sensitivity analysis showed practically no difference in flood extent across grid resolutions in the coastal area from 20 m down to 5 m, while the T_{sim}/T_{com} was consistently much greater than 6 across all simulations. In operational use, the model must run substantially faster than real time to support decision-making and repeated forecast updates; here, we adopt $T_{sim}/T_{com} < 6$ as a pragmatic criterion. Therefore, a mesh spacing of 10 m in urban areas and stream channels, and 50 m elsewhere, is a suitable compromise between accuracy and runtime effectiveness for operational modelling with a forecast scope.

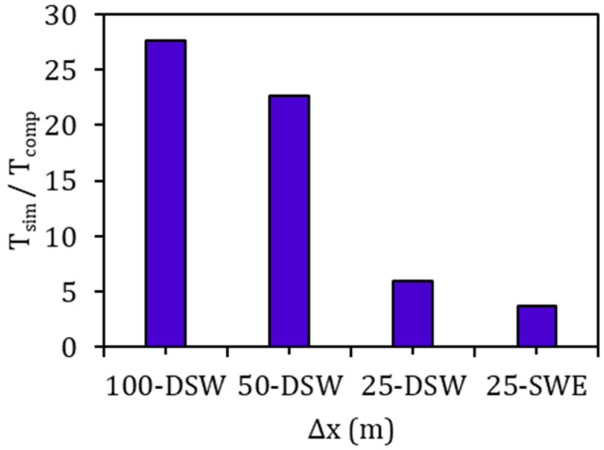

Figure 7. Ratio of simulation duration (48 h) to computational time for the different mesh resolutions. The equation set used in each simulation is also indicated.

4. Conclusions

This study presents a two-dimensional hydraulic modelling framework based on the rain-on-grid approach for simulating flash and compound flooding in a coastal urban basin with non-perennial rivers. The model integrates rainfall-driven runoff with coastal water-level forcing within a unified HEC-RAS 2D environment, aiming to support operational flood forecasting.

The results show good agreement with the Flood Risk Management Plan flood extents for precipitation-driven flooding, while identifying additional inundated areas associated with lower-order streams and direct rainfall accumulation. Coastal flooding simulations are largely consistent with official maps but yield more confined inundation due to the inclusion of buildings and the use of a fully hydraulic approach instead of a static bathtub method. The compound flooding scenario indicates a 21% increase in inundated areas compared to rainfall-only conditions, affecting both coastal and inland urban zones.

Grid sensitivity analysis indicates that a mixed-resolution mesh, combining fine resolution in urban areas and stream channels with coarser resolution elsewhere, provides an effective balance between accuracy and computational efficiency, making the proposed framework suitable for operational flood modelling.

Author Contributions: Conceptualization, A.K., C.V.M., Y.N.K. and T.K.; methodology, A.K., C.V.M. and Z.M.; software, A.K. and C.V.M.; validation, A.K., Z.M. and C.V.M.; formal analysis, A.K., C.V.M. and Y.A.; investigation, A.K., C.V.M., Y.A. and Z.M.; resources, A.K., C.V.M., Z.M. and I.P.; data curation, A.K., C.V.M., Y.A., Z.M. and I.P.; writing—original draft preparation, A.K. and C.V.M.; writing—review and editing, A.K., C.V.M., Y.A., Z.M., I.P., T.K. and Y.N.K.; visualisation, A.K.; supervision, C.V.M., Y.A., T.K. and Y.N.K.; project administration, T.K.; funding acquisition, C.V.M. and T.K. All authors have read and agreed to the published version of the manuscript.

Funding: This research is co-financed by the EU and national funds under the European Programme Interreg Euro-MED (Project 0200814 LocAll4Flood).

Institutional Review Board Statement: Not applicable.

Informed Consent Statement: Not applicable.

Data Availability Statement: The data presented in this study are available upon request from the authors.

Conflicts of Interest: The authors declare no conflicts of interest.

References

1. Morsy, M.M.; Goodall, J.L.; O'Neil, G.L.; Sadler, J.M.; Voce, D.; Hassan, G.; Huxley, C. A Cloud-Based Flood Warning System for Forecasting Impacts to Transportation Infrastructure Systems. *Environ. Model. Softw.* **2018**, *107*, 231–244. [CrossRef]
2. Ongdas, N.; Akiyanova, F.; Karakulov, Y.; Muratbayeva, A.; Zinabdin, N. Application of HEC-RAS (2D) for Flood Hazard Maps Generation for Yesil (Ishim) River in Kazakhstan. *Water* **2020**, *12*, 2672. [CrossRef]
3. Shustikova, I.; Domeneghetti, A.; Neal, J.C.; Bates, P.; Castellarin, A. Comparing 2D Capabilities of HEC-RAS and LISFLOOD-FP on Complex Topography. *Hydrol. Sci. J.* **2019**, *64*, 1769–1782. [CrossRef]
4. David, A.; Schmalz, B. Flood hazard analysis in small catchments: Comparison of hydrological and hydrodynamic approaches by the use of direct rainfall. *J. Flood Risk Manag.* **2020**, *13*, e12639. [CrossRef]
5. Ennouini, W.; Fenocchi, A.; Petaccia, G.; Persi, E.; Sibilla, S. A Complete Methodology to Assess Hydraulic Risk in Small Ungauged Catchments Based on HEC-RAS 2D Rain-On-Grid Simulations. *Nat. Hazards* **2024**, *120*, 7381–7409. [CrossRef]
6. Godara, N.; Bruland, O.; Alfredsen, K. Simulation of Flash Flood Peaks in a Small and Steep Catchment Using Rain-on-Grid Technique. *J. Flood Risk Manag.* **2023**, *16*, e12898. [CrossRef]
7. Costabile, P.; Costanzo, C.; Ferraro, D.; Barca, P. Is HEC-RAS 2D Accurate Enough for Storm-Event Hazard Assessment? Lessons Learnt from a Benchmarking Study Based on Rain-on-Grid Modelling. *J. Hydrol.* **2021**, *603*, 126962. [CrossRef]
8. David, A.; Schmalz, B. A Systematic Analysis of the Interaction between Rain-on-Grid-Simulations and Spatial Resolution in 2D Hydrodynamic Modeling. *Water* **2021**, *13*, 2346. [CrossRef]
9. Zeiger, S.J.; Hubbart, J.A. Measuring and Modeling Event-Based Environmental Flows: An Assessment of HEC-RAS 2D Rain-on-Grid Simulations. *J. Environ. Manag.* **2021**, *285*, 112125. [CrossRef] [PubMed]
10. Godara, N.; Bruland, O.; Alfredsen, K. Comparison of Two Hydrodynamic Models for Their Rain-on-Grid Technique to Simulate Flash Floods in Steep Catchment. *Front. Water* **2024**, *6*, 1384205. [CrossRef]
11. Androulidakis, Y.; Makris, C.; Kolovoyiannis, V.; Kombiadou, K.; Krestenitis, Y.; Kartsios, S.; Pytharoulis, I.; Baltikas, V.; Mallios, Z. Operational platform for metocean forecasts in Thermaikos Gulf (Aegean Sea, Greece). *J. Oper. Oceanogr.* **2025**, *18*, 123–149. [CrossRef]
12. 1st Revision of the Flood Risk Management Plan (FRMP)_for the River Basin Distrcit of Central Macedonia (EL10); General Secretariat for the Natural Environment and Water General Directorate For Water. Available online: https://floods.ypeka.gr/wp-content/uploads/2025/05/EL10_SDKP_1st_REV.pdf (accessed on 1 March 2026).
13. Makris, C.; Mallios, Z.; Androulidakis, Y.; Krestenitis, Y. CoastFLOOD: A High-Resolution Model for the Simulation of Coastal Inundation Due to Storm Surges. *Hydrology* **2023**, *10*, 103. [CrossRef]
14. Directive 2007/60/EC of the European Parliament and of the Council. Official Journal of the European Union. Available online: https://eur-lex.europa.eu/legal-content/EN/TXT/PDF/?uri=CELEX:32007L0060 (accessed on 1 March 2026).

15. Urban Hydrology for Small Watersheds; US Department of Agriculture, Soil Conservation Service, Engineering Division. Available online: https://www.nrc.gov/docs/ML1421/ML14219A437.pdf (accessed on 1 March 2026).
16. USACE HEC-RAS Hydraulic Reference Manual Version 6.6. Available online: https://www.hec.usace.army.mil/confluence/rasdocs/ras1dtechref/latest (accessed on 1 March 2026).